Environmental Science & Technology

pubs.acs.org/est

Critical Review

Recent Update on UV Disinfection to Fulfill the Disinfection Credit Value for Enteric Viruses in Water

Nicolas Augsburger, Andri Taruna Rachmadi, Noor Zaouri, Yunho Lee, and Pei-Ying Hong*

Cite This: *Environ. Sci. Technol.* 2021, 55, 16283−16298

Read Online

ACCESS | Metrics & More | Article Recommendations | Supporting Information

ABSTRACT: Ultraviolet (UV) radiation alone or in combination with other oxidation processes is increasingly being considered for water disinfection because of stringent regulatory requirements for pathogen inactivation. To fulfill this requirement, an appropriate UV dose or fluence (mJ/cm^2) is applied to combat enteric viruses in surface or treated water. There is a need for a cumulative review on the effectiveness of current and emerging UV technologies against various types of human enteric viruses. We extracted the kinetics data from 52 selected experimental studies on enteric virus inactivation using low pressure (LP-UV), medium pressure (MP-UV), UV-LED, and advanced oxidation processes (AOPs) and applied a simple linear regression analysis to calculate the range of UV fluence (mJ/cm^2) needed for 4-log$_{10}$ inactivation. The inactivation of adenoviruses with LP-UV, MP-UV, and UV/H_2O_2 (10 mg/L) required the highest fluence, which ranged from 159 to 337, 45, and 115 mJ/cm^2, respectively. By contrast, when using LP-UV, the inactivation of other enteric viruses, such as the Caliciviridae and Picornaviridae family and rotavirus, required fluence that ranged from 19 to 69, 18 to 43, and 38 mJ/cm^2, respectively. ssRNA viruses exhibit higher sensitivity to UV radiation than dsRNA and DNA viruses. In general, as an upgrade to LP-UV, MP-UV is a more promising strategy for eliminating enteric viruses compared to AOP involving LP-UV with added H_2O_2 or TiO_2. The UV-LED technology showed potential because a lower UV fluence (at 260 and/or 280 nm wavelength) was required for 4-log$_{10}$ inactivation compared to that of LP-UV for most strains examined in this critical review. However, more studies evaluating the inactivation of enteric viruses by means of UV-LEDs and UV-AOP are needed to ascertain these observations.

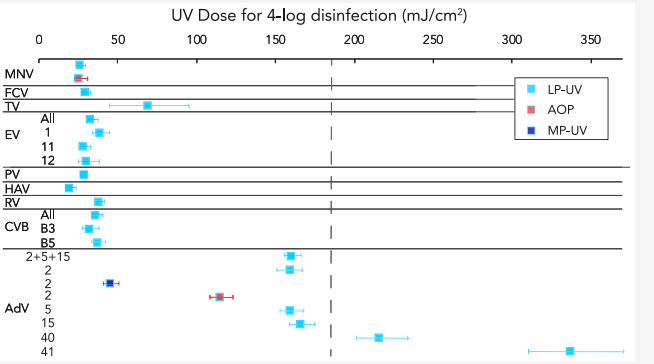

KEYWORDS: *Ultraviolet, 4-log$_{10}$ inactivation, Advanced oxidation processes, UV-LED, RNA virus, DNA virus*

1. INTRODUCTION

One of the 2016 United Nations sustainable development goals (SDG 6) is to provide universal and equitable access to clean and safe water as well as substantially increasing safe reuse globally by 2030.[1] To achieve SDG 6, water and wastewater treatment plays a critical role in removing undesirable microbial pathogens from contaminated water so that the water is safe for consumption or reuse. Some examples of microbial pathogens to remove include adenovirus, calicivirus (including norovirus), enterovirus (including polioviruses, coxsackievirus, and echovirus), and hepatitis A virus, all of which are listed in Contaminant Candidate List (CCL 4) by the United States Environmental Protection Agency (USEPA). The inclusion of these viral pathogens in CCL 4 suggests that they are known or anticipated to occur in public water systems.[2] Given their small sizes (ca. nanometers), viruses cannot be completely removed through the physical and biological processes commonly used in water and wastewater treatment systems.[3,4] However, in the case of indirect potable wastewater reuse, a cumulative 12-log$_{10}$ removal of viruses is required in California.[5,6] Hence, an effective disinfection step remains important as the last barrier to inactivate viruses that may be present in water matrices.

The disinfection methods widely used for water and wastewater treatment include chlorine and its derivatives (e.g., chloramine and chlorine dioxide), ozone, and ultraviolet (UV) radiation.[7,8] Chlorinating water containing organic matter, anthropogenic contaminants, or halogens could give rise to disinfection byproducts (DBPs) that are harmful.[9,10] Similarly, ozone is an effective oxidant but also produces toxic DBPs (e.g., bromoform, bromoacetic acid, and bromate) in water with sufficient levels of bromide (e.g., desalinated waters or municipal wastewaters in areas that rely on desalinated potable water).[11−14] By contrast, UV disinfection has attracted increasing interest since it has been demonstrated to be

Received: May 12, 2021
Revised: November 23, 2021
Accepted: November 24, 2021
Published: December 9, 2021

effective against the (oo)cysts of *Cryptosporidium* and *Giardia*, both of which are highly resistant to chlorination.[13] Furthermore, unlike chlorine, UV is not pH dependent and produces negligible amounts of toxic DBPs.[15]

Ultraviolet disinfection (UV) typically works within the germicidal range of 200−300 nm wavelengths. Low pressure UV (LP-UV) mercury lamps emit monochromatic light at 254 nm, near the wavelength range at which nucleic acids exhibit an absorption maximum, making them efficient at disinfection. UV irradiation damages the nucleic acids (DNA/RNA) of the cell or virus, primarily through the formation of pyrimidine dimers but also by other photoproducts of nucleic acids and nucleic acid lesions.[16−18] If the damage is not repaired in time, replication and transcription are blocked, in turn leading to the inactivation of microorganisms.[16,17] By contrast, medium pressure UV (MP-UV) lamps emit a range of wavelengths, including those that are absorbed by proteins and have the potential to damage the viral coat and core proteins in addition to the dimerization of pyrimidines in genomes.[16] Regardless of the type of lamp, the long-term 2 Enhanced Surface Water Treatment Rule (LT2ESWTR) recommends a UV dose of 186 mJ/cm^2 to achieve viral activation at 4-log$_{10}$.[19] The German Gas and Water Association (DGVW), New Zealand (DWSNZ), and Austrian standard institutes (ONORM) require a UV system to continuously deliver a minimum germicidal fluence of 40 mJ/cm^2.[20−23] The same UV fluence value of 40 mJ/cm^2 is applied in the Canada water supply system, although it is usually combined with chlorine disinfection.[24] This UV fluence is also recommended by the U.S. National Sanitation Foundation (NSF) in its ANSI 55 protocol to serve as primary disinfection of bacteria, viruses, and cysts in contaminated water that could be pathogenic (Class A systems). The same protocol also recommends a lower fluence of 16 mJ/cm^2 to serve as secondary disinfection of water (Class B systems).[25]

Given recent advancements in UV-based disinfection technologies, the aim of this critical review is to determine the UV fluence required for a 4-log$_{10}$ reduction of enteric virus in water using low pressure (LP) and medium pressure (MP) UV lamps and to assess the performance of emerging photocatalytic treatments using UV. The proposed fluence will be generated by applying a standard Chick−Watson linear regression model to data sets that were selected using specific criteria from earlier published studies. In addition, we recognize recent trends in UV-based technologies. Specifically, the combination of UV with oxidative radical promoters (e.g., H_2O_2, TiO_2), which are otherwise referred to as advanced oxidation process (AOP) technology, is attracting interest toward facilitating the removal of chemicals and biological contaminants from different water types, for example, drinking water or municipal wastewaters.[26] AOP forms strong oxidants, for example, •HO radicals, and it can be achieved by simultaneously applying oxidants (e.g., hydrogen peroxide, H_2O_2[27]) or photocatalysts (e.g., TiO_2)[28] in combination with UV. The presence of radical species can be useful for targeting pathogens with high resistance to UV alone.[29] Similarly, UV-LEDs are an emerging UV technology that may be suitable for point-of-use disinfection. Although studies detailing the inactivation efficiency of UV-AOP and UV-LEDs remain limited in number to permit a regression analysis, this critical review addresses some of the recent papers describing the inactivation efficacy of enteric viruses by both UV-AOP and UV-LEDs. This approach provides perspectives on whether these advances in UV disinfection approaches would be beneficial for improved removal of enteric viruses from water matrices.

2. METHODOLOGY: DATA COLLECTION, SCREENING, AND ANALYSIS WITH META-ANALYSIS

The data sets were selected according to the 2015 PRISMA-P meta-analysis protocols.[30] These data sets followed the listed criteria: (1) peer-reviewed articles excluding review papers, dissertations, online documents or reports, proceedings of a conference or meeting, (2) peer-reviewed articles containing original inactivation data from original experiments conducted by the authors and published from 1984 to January 2020 and written in English, (3) publications in which an LP-UV or MP-UV lamp was used as the UV source, with the calculated fluence determined by using a collimated beam apparatus, (4) experimental data included obtained from water-related (buffer, treated water, or reclaimed water) experiments, (5) a combination of UV fluence (the product of UV irradiance and contact time) and log$_{10}$ reduction values (LRVs) from a standard inactivation study using cell culture-based experiments, preferably a plaque assay based calculation because these assays exhibit higher sensitivity than comparable cell culture data when integrated, (6) inactivation data sets excluded without clear protocol descriptions and details pertaining to the cell line host and/or qPCR, and (7) long-range qPCR or RT-PCR or a combination of integrated cell culture data only included if shown to be comparable to cell culture infectivity-based methods but excluded when the authors demonstrate significant differences between the quantification methods.[31,32] The kinetics of the virus infectivity and UV dose were calculated using the Chick−Watson model described in the following formula

$$\mathrm{Log}_{10}\left(\frac{N_t}{N_0}\right) = -kF \tag{1.1}$$

where Nt is the virus concentration at specific sampling times, N_0 the initial concentration of the viruses at time zero, k the inactivation rate constant by UV (cm^2/mJ), and F the UV fluence or dose (mJ/cm^2).

Data sets published from 1984 to 2020 were obtained from the NCBI and Google Scholar databases. In the literature, UV fluence and dose are at times used interchangeably to refer to the same concept. Hence, the keywords used for the search were "UV" + "kinetics OR fluence dose OR dose response" + "virus type", including "human norovirus" (HuNoV), "adenovirus" (AdV), "echovirus" (EV), "coxsackie B virus", (CVB), "poliovirus (PV)", hepatitis A virus" (HAV), and "human rotavirus" (HRV). Murine norovirus (MNV), feline calicivirus (FCV), and Tulane virus (TV) were included as surrogates for human norovirus due to the unavailability of robust cell lines for human norovirus infectivity assays.[33] All the listed viruses except rotavirus were chosen for this critical review because they are listed as viral contaminants in the Microbial Contaminants − CCL 4.[34] Although rotavirus is not on the CCL 4 list, it is included in this critical review because it has a common etiology responsible for diarrhea incidence and mortality in children younger than 5 years old.[35] After the initial screening results were obtained, each paper's title and abstract were cross-checked to ensure that the paper fulfilled all the requirements mentioned above. Duplicate papers found in both databases were also eliminated. The data were extracted

https://doi.org/10.1021/acs.est.1c03092
Environ. Sci. Technol. 2021, 55, 16283−16298

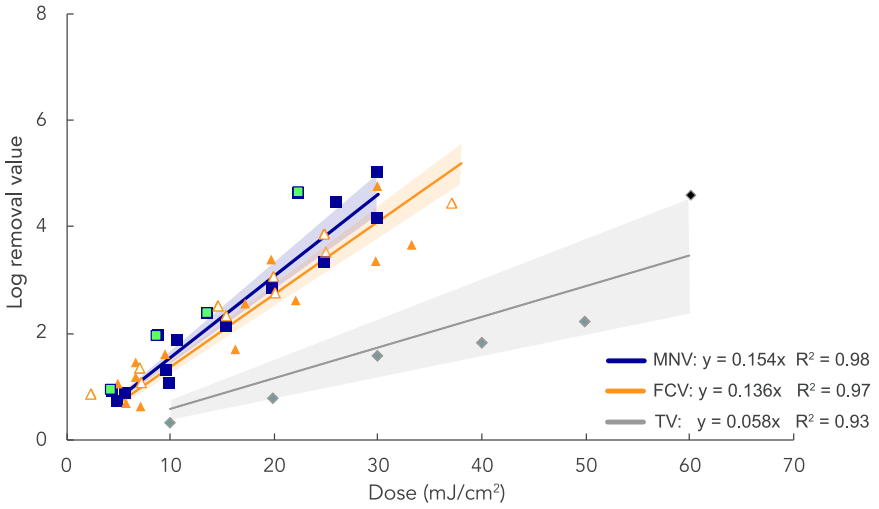

Figure 1. Standard linear regression models for LP-UV inactivation of Caliciviridae. Blue squares, orange triangles, and gray diamonds represent the data sets for murine norovirus (MNV),[38−40] feline calicivirus (FCV),[38,41] and Tulane virus (TV),[42] respectively. Closed shapes represent buffered matrices, while green- and white-filled data points signify data from municipal wastewater and drinking water, respectively. The regression slopes for MNV, FCV, and TV are described with blue, orange, and gray lines, respectively. The 95% confidence interval is indicated by the shaded area. The black-filled diamond represents a data point that reached the limit of quantification,[42] and the dashed gray line represents the linear regression omitting this point.

from the articles by a single reviewer (name initials: A.T.R.) and verified by another reviewer (name initials: N.A.). The extracted data included the UV dose, LRVs, tested virus strains, virus detection methods, experimental conditions of the water matrices (pH, turbidity, and temperature), and correction factors.

Two methods were employed to extract the UV and LRV doses. First, when the UV dose was available in the selected paper, the values specified in the manuscript were directly used either by first digitalizing the plots or from the original data provided in tabular format. Second, in experiments in which the UV lamp irradiance (in Watt/area) and inactivation time were available in the manuscript, including the Supporting Information, manual calculations were conducted to obtain the UV fluence by multiplying the irradiance by the exposure time and assuming no absorbance by the water matrices

$$F = I \times t \tag{1.2}$$

where I is the fluence rate of the UV lamp (mW/cm^2), and t is the exposure time in units of seconds.

Table S1 summarizes whether data extracted from the papers have accounted for absorbance of the water matrices when calculating the fluence or whether the experiments were carried out under thin film conditions (<1 cm). Correction factors from experiments using nonbuffered matrices or purified water are further detailed in Table S2. Most corrected irradiances were based on Bolton and Linden,[36] which account for UV absorption, water depth, and some included reflection off the water surface and the nonuniform distribution of light across the sample. Moreover, all the MP-UV studies determined the average irradiance by measuring the irradiance in the germicidal range of 200−300 nm, which is weighted based on the DNA absorbance spectrum as previously described by Linden and Darby[37] and using the previously mentioned Bolton and Linden[36] correction factors. The extracted UV doses and LRVs from the selected articles were collated together for the same virus species and serotype. A Chick−Watson linear regression was used to generate the slope coefficient (k) to calculate the UV dose for 4-log$_{10}$ virus inactivation. In the regression models, LRV was used as a dependent variable, and UV fluence was the independent variable. Correlation parameters, including the slope, intercept, and 95% confidence interval range, were generated as the output, and based on the Chick-Watson results, the y-intercept was assumed to be 0. For data sets with tailing phenomena, only exponential decay was considered for the kinetic analysis. All the linear regressions resulted in an R^2 higher than or equal to 0.93. Variance values among residuals to fitted values were compared, and the adjusted determination coefficient (R^2) was also calculated. While Chick−Watson linear regression was suggested for 4-log$_{10}$ virus inactivation in this critical review, a simple linear regression model in which the y-intercept was not assumed to be 0 was also performed (Tables S3−S5) to account for shouldering effects but was not used in the comparative analysis discussed in this critical review.

For instances in which the slopes of the regression model parameters showed no significant differences between different genotypes/serotypes of a virus type as tested by ANCOVA, data sets derived from different genotypes/serotypes within the same virus were combined in the regression analysis. In brief, for the covariance analysis, a linear ANOVA model was generated with log$_{10}$ removal as the response, with the different serotypes, water matrices, detection methods, or authors as the factors and the fluence (mJ/cm^2) as the covariates. After the linear model was established, pairwise comparisons were made using the Tukey method and using the serotype or specified condition as the term for pairwise comparison to generate an ANCOVA-adjusted p-value between the tested groups and factors. All modeling and statistical analyses were conducted using Microsoft Excel and Minitab for linear regressions and ANCOVA, respectively.

In total, more than 29,000 articles were considered, and based on the title and abstract content, 543 articles were verified for further screening through the employed criteria. Ninety-four articles were chosen after the initial screening. In the end, for the LP-UV data sets, we narrowed down the references to three articles on MNV,[38−40] two articles on

https://doi.org/10.1021/acs.est.1c03092
Environ. Sci. Technol. 2021, 55, 16283−16298

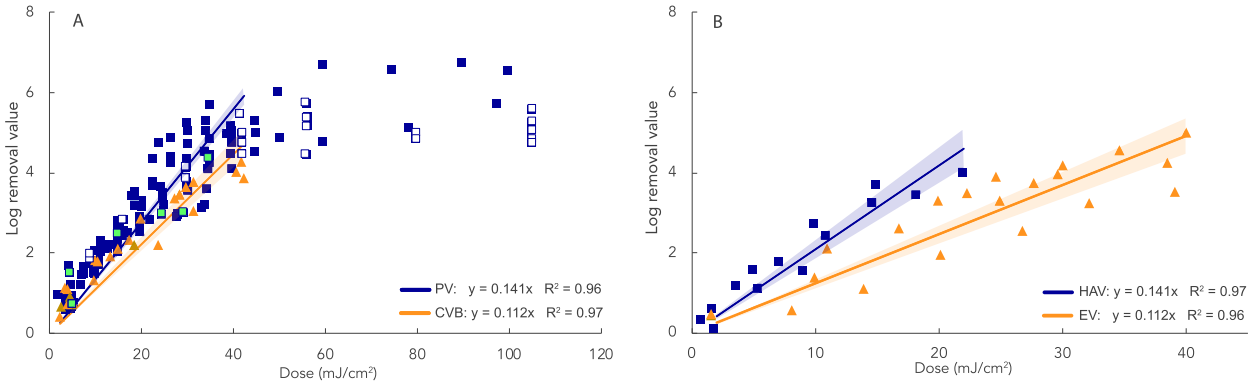

Figure 2. Standard linear regression models for LP-UV inactivation of Picornaviridae. (A) Blue squares and orange triangles represent the data sets for poliovirus PV[43−52] (PV) and CVB (B3[44] + B5[44,53]), respectively. Closed shapes represent buffered matrices, while green- and white-filled data points signify data from municipal wastewater and drinking water, respectively. The regression slopes for PV and CVB are described with blue and orange lines, respectively. All the CVB serotypes were included as a single regression due to a lack of significant differences, and the tailing effect from 40 mJ/cm^2 was not included in the linear regression. (B) Blue squares and orange triangles represent the data sets for hepatitis A (HAV[39]) and echovirus EV (1,[44] 11,[44] 12[38]), respectively. The regression slopes for HAV and EV are described with blue and orange lines, respectively, in which there was no significant difference based on the EV serotype, and they were therefore modeled by a single linear regression. The 95% confidence interval is indicated by the shaded area.

FCV,[38,41] one article for TV,[42] 10 articles for PV,[43−52] one article for HAV,[53] five articles for HRV,[31,43,51,53,54] two articles for EV,[38,44] three articles for CVB,[44,47,53] and 14 articles for AdV.[17,29,32,41,44,50,55−62] For MP-UV, five studies related to adenovirus serotype 2[17,56,57,60,63] were selected for data analysis. Regarding the UV-AOP studies, one paper for inactivation by UV + H_2O_2 for both adenovirus serotype 2[29] and one paper regarding UV + TiO_2 inactivation using MNV[40] were extracted. Regarding UV-LEDs, four studies[49,63−65] included the inactivation of AdV,[63,64] FCV,[65] EV,[49] enterovirus,[49] PV,[49] and CVB.[49] The papers that fulfilled our selection criteria used phosphate buffer solution (PBS), minimal essential media MEM, buffered demand-free (BDF) water, purified water, drinking water, groundwater, and treated wastewater as matrices for the virus inactivation studies. The significances of the groups, water matrices, and detection methods in all the data sets in which there was more than one water matrix used for a given serotype are further detailed in Tables S6−S8.

3. RESULTS

3.1. Enteric Virus Inactivation Using LP-UV. LP-UV generates monochromatic irradiation in the UV-C region with a peak wavelength of 253.7 nm. Within the Caliciviridae family (nonenveloped, single-stranded RNA), inactivation studies using LP-UV were conducted on murine norovirus (MNV), Tulane virus (TV), and feline calicivirus (FCV) as human norovirus HuNoV surrogates (Figure 1). The Chick−Watson-based linear regression showed correlation coefficient (k) values of 0.154, 0.136, and 0.058 with R^2 values of 0.98, 0.97, and 0.93 for MNV, FCV, and TV, respectively (Figure 1). TV was significantly more persistent in response to LP-UV than both MNV and FCV (ANCOVA p-value < 0.001), while MNV and FCV were not significantly different (ANCOVA p-value = 0.558). Specifically, the mean UV doses required for 4-log$_{10}$ reduction of MNV, FCV, and TV are 26, 29, and 69 mJ/cm^2, respectively.

LP-UV data were also collected for the Picornaviridae family (nonenveloped single-stranded RNA), namely, poliovirus (PV), coxsackievirus (CVB), echovirus (EV), and hepatitis A (HAV) (Figure 2). Poliovirus and hepatitis A data set analyses by linear regression revealed coefficient correlation k-values of 0.141 and 0.99 with R^2 values of 0.96 and 0.99, respectively, and the mean required doses were 28 and 16 mJ/cm^2. LP-UV disinfection of PV resulted in a significant tailing effect beginning at 50 mJ/cm^2 which is after the mean required dose of 28 mJ/cm^2. The two viruses within Picornaviridae with various serotypes were coxsackievirus and echovirus. The sensitivities of CVB 3 and CVB 5 to UV radiation were not significantly different (ANCOVA p-value = 0.63), nor was echovirus 1, 11, and 12, with ANCOVA p-values of 0.422, 0.934, and 0.33 when comparing 1 vs 11, 1 vs 12, and 11 vs 12, respectively. Considering that the CVB and EV serotypes were collated due to statistical insignificance, the required doses for 4-log$_{10}$ reduction were 36 and 33 mJ/cm^2, respectively. All the calculated doses within the 95% confidence are listed in Table 1.

Rotaviruses of the family Retroviridae, which have double-stranded (ds)RNA segments as their genome, showed a level of resistance with evident tailing after 50 mJ/cm^2 (Figure 3). To avoid giving a false sense of persistence, only exponential decay was used for the linearly fit model. The mean slope coefficient was 0.107, and R^2 was 0.97. This linear regression resulted in a prediction of a 38 mJ/cm^2 dose to achieve a 4-log$_{10}$ reduction, and the doses within 95% confidence are listed in Table 1. However, the tailing effects for rotavirus are particularly relevant, because this added persistence begins around the 4-log$_{10}$ reduction mark.

Adenovirus, a double-stranded DNA virus, is the most resistant to UV radiation compared to all the enteric viruses. The AdV data sets included in this study were categorized based on different serotypes, in which AdV2, 5, 15, 40, and 41 were analyzed (Figure 4). The k-values generated from the linear regression for all AdV strains were 0.025, 0.025, 0.024, 0.019, and 0.012, with R^2 values of 0.95, 0.98, 1.00, 0.97, and 0.93, respectively (Figure 4). Serotypes 40 and 41 were significantly different from the others and from each other (ANCOVA p-values < 0.001 for 40 vs 2 and 41 as well as 41 vs 2, 5, and 15 with 40 vs 5 = 0.005 and 40 vs 15 = 0.002). However, AdV2, 5, and 15 were not significantly different from each other (ANCOVA p-values of 1.0 for 2 vs 15, 0.085 for 2 vs 5, and 0.661 for 5 vs 15). The difference in kinetics is

https://doi.org/10.1021/acs.est.1c03092
Environ. Sci. Technol. 2021, 55, 16283−16298

Table 1. Summary of UV Doses needed for 4-$\log_{10}$ Reduction in mJ/cm^2 for All Analyzed Viruses Using LP-UV [MNV,[38−40] FCV,[38,41] TV,[42] EV(1,[44] 11,[44] 12[38]), CVB(B3,[44] B5[44,53]), PV,[43−52] HAV,[53] HRV,[31,43,51,53,54] and AdV(2,[17,29,44,50,55−60] 5,[58,61] 15,[50] 40,[41] 41[32,58,62])][a]

Enteric Virus	Strain	LP-UV dose needed for 4-log reduction (mJ/cm^2)					
		Upper bound	**Mean (F)**	Lower bound	k (cm^2/mJ)	R^2	Adjusted R^2
MNV	MNV-1	28	**26**	24	0.154	0.98	0.91
FCV	NA	32	**25**	22	0.136	0.97	0.93
Tulane Virus	Na	100	**69**	53	0.058	0.93	0.73
Echovirus	All Echo	36	**33**	39	0.122	0.96	0.91
	Echo 1	44	**38**	34	0.104	0.98	0.85
	Echo 11	30	**28**	25	0.144	0.99	0.85
	Echo 12	36	**30**	25	0.135	0.99	0.66
Coxsackievirus	All cox	40	**38**	33	0.112	0.97	0.94
	B3	37	**32**	28	0.127	0.98	0.81
	B5	41	**37**	34	0.108	0.97	0.91
Poliovirus	PV-1	30	**28**	27	0.141	0.96	0.95
Hepatitis A	HM-175	20	**16**	13	0.257	0.99	0.49
Rotavirus	SA-11	40	38	35	0.107	0.97	0.94
Adenovirus	AdV 2+5+15	165	**160**	156	0.025	0.96	0.96
	AdV 2	165	**159**	153	0.025	0.95	0.95
	AdV 5	166	**159**	153	0.25	0.98	0.96
	AdV 15	173	**166**	159	0.024	1.00	0.91
	AdV 40	232	**216**	201	0.019	0.97	0.93
	AdV 41	369	**337**	310	0.012	0.93	0.91

[a]The doses (mJ/cm^2) were calculated based on eq 1.1: $\mathrm{Log}_{10}(N_t/N_0) = -kF$ (in which the y-intercept is assumed to be 0). The lower and upper bounds are based on 95% confidence intervals in terms of suggested fluence. Both the R^2 and the adjusted R^2 are also listed. Light blue, gray, and light orange shadings indicate single-stranded RNA, double-stranded RNA, and double-stranded DNA viruses, respectively.

exemplified by the required doses (mJ/cm^2) for the 4-$\log_{10}$ removal of each serotype. In the AdV2 + 5 +15 group, 40, and 41 were 160, 216, and 337 mJ/cm^2, respectively, and the required doses based on the 95% intervals are listed in Table 1. Within our search criteria, adenovirus serotype 2 had received the most attention in the literature, including 10 papers compared to the 2, 1, 1, and 3 papers found for AdV5, 15, 40, and 41, respectively. However, AdV2 was among the most sensitive of the serotypes, while AdV41 was the most resistant virus included in this critical review, requiring more than double the LP-UV dose compared to AdV2.

3.2. Enterovirus Inactivation Using MP-UV. In contrast to LP-UV, MP-UV emits a broad range of wavelengths that are also capable of leading to cellular damage and ultimately to inactivation at less than half the fluence (i.e., based on AdV2 shown in Tables 1 and 2). Due to the broader spectrum of MP-UV lamps, they will lead to enhanced damage to critical proteins, enzymes, and other microbial constituents in addition to nucleic acid damage and may also limit or prevent photoreactivation in neutral pH and at room temperature.[16,66] Photoreactivation is a natural process in which cells can partially recover from ultraviolet damage when visible and UV wavelengths of light reverse DNA damage by monomerizing cyclobutene pyrimidine dimers, but this is unlikely to happen in RNA viruses due to the lack of a cell host repair mechanism in RNA viruses.[66]

Among all the known enteric viruses, only AdV, TV, and HRV inactivation data using MP-UV are currently published. However, this critical review only included a regression analysis for data derived from exposing AdV2 because it includes consideration of typical broad range MP-UV as well as the aforementioned selection criteria. Data sets for adenovirus serotype 2 were obtained from five papers using broad range MP-UV.[17,56,57,60,63] Overall, MP-UV provided a significant

https://doi.org/10.1021/acs.est.1c03092
Environ. Sci. Technol. 2021, 55, 16283−16298

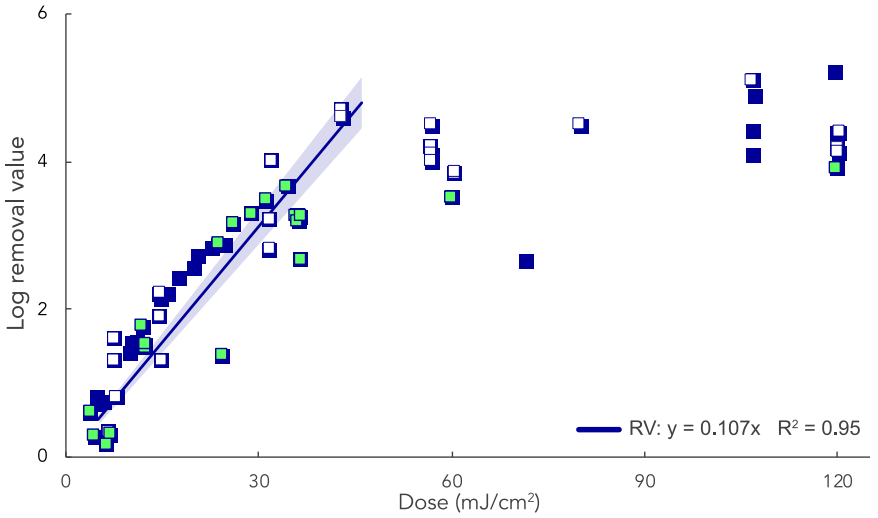

Figure 3. Standard linear regression models for LP-UV inactivation of rotavirus[31,43,51,53,54] where the tailing effect from 50 mJ/cm^2 was not included in the linear regression. Closed shapes represent buffered matrices, while green- and white-filled data points signify data from municipal wastewater and drinking water, respectively. The regression slope is described with a blue line, and the 95% confidence interval is indicated by the shaded area.

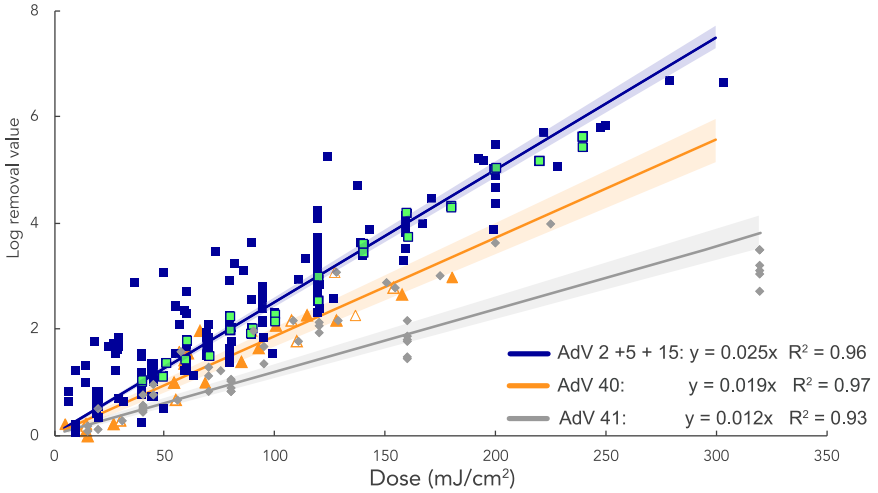

Figure 4. (A) Standard linear regression models for LP-UV inactivation of adenovirus 2[17,29,44,50,55−60] + 5[58,61] + 15[50] (not significantly different), AdV40,[41] and AdV41.[32,58,62] Blue squares, orange triangles, and gray diamonds represent extracted data, while linear regressions are described with blue, orange, and gray lines for AdV2 + 5, 40, and 41, respectively. The 95% confidence interval is indicated by the shaded area. Closed shapes represent buffered matrices while green- and white-filled data points signify data from municipal wastewater and drinking water, respectively.

Table 2. UV Dose Needed for 4-log$_{10}$ Reduction in mJ/cm^2 for All Analyzed Viruses When Using MP UV (AdV2[17,56,57]) and AOP (MNV,[40] AdV2[29])[a]

Enteric Virus	Strain	Treatment	Condition	UV dose needed for 4-log reduction (mJ/cm^2)					
				Upper bound	**Mean (F)**	Lower bound	k (cm^2/mJ)	R^2	Adjusted R^2
MNV	MNV 1	LP-UV/TiO_2	10 mg/L TiO_2	30	**25**	22	0.159	0.99	0.66
Adenovirus	AdV-2	MP-UV	N/A	49	**45**	42	0.089	0.95	0.92
		LP-UV/H_2O_2	10 mg/L H_2O_2	122	**115**	108	0.035	0.98	0.94

[a]The lower and upper bounds are based on 95% confidence intervals in terms suggested fluence. The doses (mJ/cm^2) were calculated based on eq 1.1: $\mathrm{Log}_{10}(N_t/N_0) = -kF$ (in which the y-intercept is assumed to be 0). Both the R^2 and the adjusted R^2 are also listed. Light blue and light orange shading indicate single-stranded RNA and double-stranded DNA viruses, respectively.

https://doi.org/10.1021/acs.est.1c03092
Environ. Sci. Technol. 2021, 55, 16283−16298

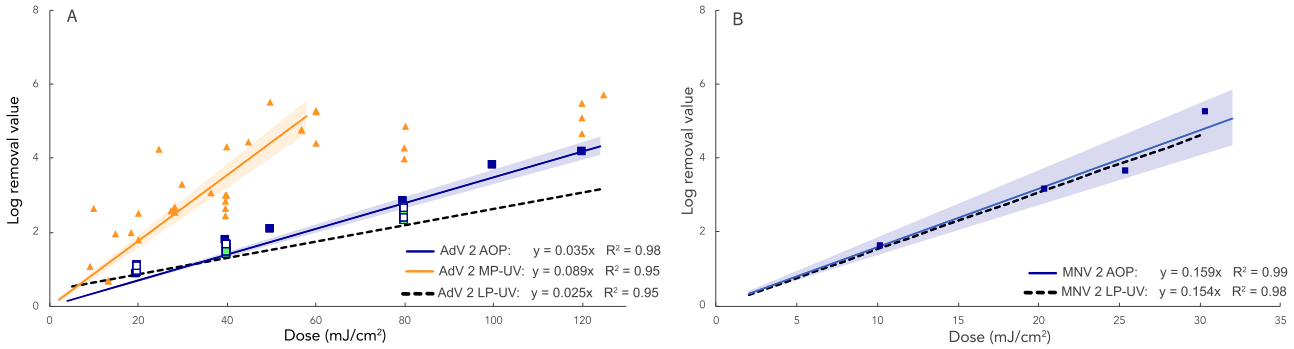

Figure 5. (A) Standard linear regression models for MP-UV[17,56,57] as represented by orange triangles and regression line. LP-UV/H_2O_2[29] is represented by blue squares and regression line, with reference to the linear regression model of LP-UV alone, all in adenovirus AdV2 only. The 95% confidence interval is indicated by the shaded area. Closed shapes represent buffered matrices while green- and white-filled data points signify data from groundwater and surface water, respectively. The papers referenced in this figure employed the germicidal weighting method for MP UV disinfection proposed by Bolton and Linden.[36] (B) Standard linear regression models for the LP-UV/TiO2 inactivation of MNV[40] represented by blue squares and the linear regression model of LP-UV disinfection. The 95% confidence interval for LP-UV/TiO_2 is indicated by the shaded area.

Table 3. UV Dose Needed for 4-log_{10} Reduction in mJ/cm^2 for All Analyzed Viruses When Using LED[49,63−65,a]

Enteric Virus	Strain	Wavelengths	UV dose needed for 4-log reduction (mJ/cm^2)					
			Upper bound	**Mean (F)**	Lower bound	k (cm^2/mJ)	R^2	Adjusted R^2
FCV	-	265 nm	35	**32**	29	0.126	1.00	0.66
		280 nm	40	**38**	36	0.105	1.00	0.67
Echovirus	30	260 nm	82	**23**	14	0.171	0.95	0.45
		280 nm	37	**25**	19	0.158	0.99	0.49
Coxsackievirus	A10	260 nm	21	**17**	15	0.231	0.99	0.66
		280 nm	28	**21**	16	0.194	0.98	0.65
		260 + 280 nm	24	**18**	14	0.223	0.99	0.49
Poliovirus	PV-1	260 nm	21	**17**	15	0.231	0.99	0.66
		280 nm	24	**20**	16	0.205	0.99	0.66
		260 + 280 nm	20	**18**	17	0.219	1.00	0.75
Enterovirus	70	260 nm	92	**22**	13	0.178	0.94	0.44
		280 nm	87	**30**	15	0.168	0.98	0.48
		260 + 280 nm	50	**23**	15	0.173	0.97	0.47
Adenovirus	AdV-2	260 nm	135	**112**	95	0.036	0.96	0.82
		280 nm	140	**109**	89	0.037	0.94	0.80
		260 + 280 nm	152	**115**	92	0.035	0.93	0.79
	AdV-5	285 nm	184	**171**	159	0.023	0.99	0.89

[a]The doses (mJ/cm^2) were calculated based on eq 1.1: $Log_{10}(N_t/N_0) = -kF$ (in which the y-intercept is assumed to be 0). The lower and upper bounds are based on 95% confidence intervals in terms suggested fluence. Both the R^2 and the adjusted R^2 are also listed. Light blue and light orange shading indicate single-stranded RNA and double-stranded DNA viruses, respectively.

https://doi.org/10.1021/acs.est.1c03092
Environ. Sci. Technol. 2021, 55, 16283−16298

increase in the removal efficiency for adenovirus serotype 2 compared to LP-UV and LP-UV + H_2O_2 (5 and 10 mg/L), with ANCOVA p-values < 0.001. A pronounced tailing effect was observed with MP-UV inactivation, and the linear regression model should not be applied at higher fluence based on these data. When including only the exponential decay subset of data (data points up to 60 mJ/cm^2) for the Chick−Watson linear regression approach, 45 mJ/cm^2 is required to achieve a 4-log$_{10}$ reduction of AdV2 when using MP-UV (Figure 5A, Table 2).

3.3. Enteric Virus Inactivation Using UV-AOP Process and UV-LED. AOP provides an opportunity to use the high effectiveness of UV disinfection while reducing possible persistence by combining UV with specific compounds that will generate OH radicals, such as H_2O_2 and TiO_2, which are included in this critical review. OH radicals are strong oxidants that can inflict damage on components of viral particles outside of the DNA/RNA damage inflicted by LP-UV, and the results analyzed in this critical review are listed in Table 2.

AdV2 inactivation data achieved by LP-UV and LP-UV/H_2O_2 are shown in Figure 5A. Inactivation was performed in groundwater and surface water. In that study,[29] using the same Chick−Watson linear regression approach, 214 mJ/cm^2 was needed for a 4-log$_{10}$ reduction (R^2: 0.98) with LP-UV. Adding 5 and 10 mg/L H_2O_2 significantly (ANCOVA p-values 0.048 and <0.001, respectively) decreased the required UV dose to 126 and 110 mJ/cm^2, respectively, to achieve 4-log$_{10}$ inactivation in this study. OH radicals produced during the advanced oxidation process are likely able to damage parts of the virus not targeted by LP-UV, such as attachment proteins, enhancing UV-induced inactivation. However, the k-value (i.e., 0.031−0.036) obtained from this study after the addition of 5 and 10 mg/L H_2O_2 was not significantly different (ANCOVA p-values > 0.05) from the k-value obtained from the collated data (i.e., k = 0.025) that we analyzed for the LP-UV data and AdV2 in this critical review (Table 1).

In addition to the use of H_2O_2, heterogeneous AOPs using photocatalysts, such as TiO_2, are also being considered. Related research on enteric viruses was published by Lee et al.[40] (Figure 5B). In this particular study, 10 mg/L of TiO_2 was used along with LP-UV to disinfect MNV. To maximize the yield of reactive oxygen species, a TiO_2 suspension was pre-exposed to 33 mJ/cm^2 of LP-UV prior to introducing the virus. Despite this treatment, the 25 mJ/cm^2 required to achieve a 4-log$_{10}$ reduction was not significantly lower than the minimum suggested dose of 26 mJ/cm^2 from the generated linear regression model of MNV inactivation using LP-UV (Figure 1), suggesting that adding TiO_2 in this instance did not significantly enhance the inactivation efficiency.

Recently, some studies about the emerging use of ultraviolet light emitting diode (UV-LED)-based technology for pathogen inactivation have been published, although the data for enteric viruses are also very limited,[49,63−65,67−71] such as that of UV-AOP. UV-LEDs are mercury free, physically robust, and flexible in regard to the selection of emission wavelengths. Its operation also permits a faster start-up time with a potentially lower fluence requirement.[65,70] Data using wavelengths of 260, 265, 280, and 285 nm were chosen for their higher efficiencies compared to that of UV-LED technologies using wavelengths outside the germicidal range. A summary of the kinetics regarding UV-LED studies on enteric viruses is summarized in Table 3. Unlike UV-C, the emission from LEDs is not monochromatic, and only nominal peak wavelengths are reported by the authors despite LEDs emitting spectral ranges rather than a single wavelength.[49,63]

From two analyzed studies,[49,63] UV-LEDs at 260 nm required fluences of 17, 17, 23, 22, and 112 mJ/cm^2 for the 4-log$_{10}$ inactivation of coxsackievirus A (CVA), PV, EV, enterovirus 70, and adenovirus 2, respectively, while 21, 20, 25, 24, and 109 mJ/cm^2 were required for 4-log$_{10}$ inactivation at 280 nm, respectively. Furthermore, 18, 18, 23, and 115 mJ/cm^2 for a 4-log$_{10}$ inactivation of coxsackievirus A (CVA), PV, enterovirus 70, and adenovirus 2, respectively, were required using a combination of 260 and 280 nm. Overall, there were no significant differences in the inactivation performance of UV-LEDs at 260 and 280 nm or the combination of 260 and 280 nm for any of the viruses tested in these studies. Only in the case of CVA[49] was any significant difference detected based on these wavelengths, in which 260 nm significantly outperformed 280 nm (ANCOVA p-value = 0.037), but neither was significantly different from the 260 and 280 nm combination.

A separate study[64] on the inactivation of adenovirus 5 using UV-LED 285 nm showed UV fluences of 171 mJ/cm^2 to obtain 4-log$_{10}$ inactivation, which is higher than the LP-UV requirement described in this critical review (Table 1). Last, a comparison between UV-LED 265 and 280 nm treatments of feline calicivirus (FCV)[65] showed a significant benefit to using 265 vs 280 nm (ANCOVA p-value = 0.037), in which 32 and 38 mJ/cm^2 were needed for 4-log$_{10}$ inactivation, respectively. In general, UV-LED technology at 260 or 280 nm showed potential for requiring a lower UV fluence for 4-log$_{10}$ inactivation compared to LP-UV in most strains examined in this critical review. However, for more persistent enteric viruses such as adenoviruses, UV-LEDs only provided a slight improvement on LP-UV, and MP-UV still remains significantly more efficient (e.g., referring to AdV2 data in Tables 1, 2, and 3).[63]

Despite the promise of UV-LEDs for virus inactivation, some concerns about UV-LED studies include (1) a lack of uniformity in research materials and methods for UV-LED disinfection studies, which makes comparison difficult, (2) some inconsistent results for pathogen inactivation due to various radiation patterns, such as the emission spectra, viewing angle, and radiation distribution, and (3) the absence of a standardized protocol for microorganism inactivation.[70]

4. DISCUSSION

4.1. Differences in Susceptibility to UV Disinfection among Viral Species and Serotypes. Viral inactivation is complicated by the observation that closely related viruses may exhibit different disinfection kinetics when subjected to disinfection.[72] Enteric virus susceptibility to UV radiation may differ depending on the genome size, pyrimidine content, and genome and protein sequences.[73] Prior knowledge of the capsid and genome structure in addition to the sequence will help in predicting virus particle reactivity to UV radiation.[73] In addition, UV 254 nm damage within the genome and protein varies per region. For example, in MS2 inactivation with UV, a decrease in the capsid peptide concentration was observed in six different peptides (Val44-Arg49), which undergo site-specific backbone cleavage between Ser47 and Val48 residues.[72] Likewise, on the basis of our results, there seem to be differences in susceptibility among and between Caliciviridae and Picornaviridae (both ssRNA viruses) compared to Reoviridae (dsRNA virus) and Adenoviridae

https://doi.org/10.1021/acs.est.1c03092
Environ. Sci. Technol. 2021, 55, 16283−16298

(dsDNA virus), with the dsRNA and dsDNA viruses being less susceptible to UV radiation.

TV was the most resistant to LP-UV among the Caliciviridae family members discussed in this study (Table 1). Although MNV, TV, and FCV are classified in the same family, they belong to different genera of norovirus, recovirus, and vesivirus, respectively, so their different genomes may have accounted for different susceptibilities to UV radiation.[38] A recent publication by Rockey et al. mentioned that both TV and HuNoV have similar levels of susceptibility to UV 254 nm inactivation compared to other Caliciviridae (e.g., FCV and MNV) when measured for their inactivation kinetics by qPCR.[74] Hence, TV might be a closer surrogate than MNV for determining the required UV dose needed for HuNoV inactivation. These differences showed that sensitivity to disinfectants is species/genotype/serotype specific even if they are in the same Caliciviridae family. Therefore, depending on the type of disinfectant that is to be evaluated, different surrogates, preferably the ones that are the most resistant to that type of disinfectant, should be considered to provide information on the maximum required disinfectant dose needed to achieve the desired log reduction.

Likewise, in the Picornaviridae family, there are different sensitivities to LP-UV among EV serotypes 1, 11, and 12. By contrast, there was no difference in LP-UV sensitivity between CVB3 and CVB5. The lack of difference in susceptibility may be accounted for by being in the same serotype B, and therefore, CVB3 and CVB5 share similar structures and have more than 90% genome sequence similarity.[75]

The higher resistance of rotavirus to UV compared to the Picornaviridae and Caliciviridae families may be caused by their double-stranded RNA genetic makeup, which leads to more structural stability and redundancy of information in the complementary strands.[66] The photolysis rate constant of naked nucleic acids measured by qPCR and normalized by the number of bases measured in a particular sequence revealed that naked ssRNA reacted 24 times faster than dsRNA.[76] The double-stranded RNA structure is more stable than single-stranded RNA in response to UV radiation due to hydrogen bonding within the helix structure. This structure may lead to a lower absorbance of UV radiation compared to single stranded RNA, although more comprehensive experiments should be performed to confirm this hypothesis.[53] Sensitivity to UV inactivation may also be influenced by multiplicity reactivation phenomena in which inactivated virus particles may complement each other such that reproduction can take place in host cells during multiple infections.[77,78] The damaged virus will not be able to initiate viral infection in the cells without the aid of companion virus particles; therefore, a large number of partially damaged viruses may be required for infection. In higher genome size viruses such as HRV, a greater UV dose is required to destroy the genome, possibly leading to fewer partially damaged virus particles needed for multiplicity reactivation.[53] For those reasons, it is understandable that rotavirus SA11 (>15,000 nucleotides), with its double-stranded RNA structure, has higher resistance than other single-stranded RNA viruses, such as MNV and TV (~7200 nucleotides), PV (~7300 nucleotides), and EV 11 (7438 nucleotides).

Adenoviridae, which are dsDNA viruses, have the highest resistance to UV disinfection, which may be due to their ability to repair their genome in the cell host during replication in addition to their large genome size (~34,000 nucleotides).[16,17] Among the adenovirus strains, AdV41 is the least susceptible to LP-UV compared to AdV2, 4, 5, and 40. Similar results with other disinfectants also showed gastroenteritis AdV40 and 41 to be less susceptible to UV, free chlorine, and monochloramine compared to AdV5 and other serotypes, which were less frequently associated with gastroenteritis.[58,78−80] These observed differences in susceptibilities may be due to variations in the genome sequence and protein structure that corresponded to the host binding efficiency, with serotypes associated with gastroenteritis typically showing higher host binding efficiency that can lead to a higher infection rate by the surviving viral particle after UV exposure compared to the low host binding efficiency serotype. Other factors that may influence the difference in UV sensitivity among different serotypes are different light absorptivities and photoionization quantum yields because the most reactive amino acid and nucleoside monomers varied in capsid structure serotype, although experimental confirmation should be conducted.[81,82]

When determining the inactivation rates in different virus serotypes, the use of different cell hosts to quantify the viability of viruses may have contributed partly to differences in their inactivation rates.[17] For example, the inactivation rate of AdV5 as measured by HEK 293, PLC/PRF/5, and XP17BE cell lines showed inactivation rates that ranged from 0.0264 to 0.0765. These numbers translate to a range of 52−151 mJ/cm^2 needed to achieve a 4-log$_{10}$ reduction in AdV5.[83]

4.2. Comparison between LP-UV, MP-UV, UV-LED, UV/H_2O_2, and UV/TiO_2 toward Enteric Virus Inactivation and Implications for Detection. MP-UV is polychromatic with a wide range of wavelengths, including those that are absorbed by proteins, and thus, it has the potential to disrupt the virion structure, damaging the viral capsid and core proteins in addition to the genome.[17,83] The basic structure of viruses includes a genome (single- or double-stranded RNA/DNA), a protein capsid, and sometimes an envelope.[84] Damage to the capsid means there is no protection for the virus genomic material from the outer environment and leads to loss of the infectious role of the virus due to loss of protein, which is required for attachment to the cell host, lysing endosomes, and facilitating the release of DNA into the host cell nucleus.[60,85] Unlike RNA viruses, DNA viruses such as AdV have a repair machinery that occurs in the cell host after UV treatment, so the additional damage in the AdV capsid may have accounted for the higher efficacy of MP-UV compared to LP-UV.

Different UV-C wavelengths emitted simultaneously by polychromatic MP-UV will have different efficacies toward virus inactivation. Monochromatic 254, 270, and 290 nm irradiation corresponded to adenoviral genome damage in AdV2.[60] By comparing molecular to infectivity detection methods of AdV2 detection, it was shown that more nucleic acid damage was observed than reduction in viral infectivity at 260 nm. At 240 nm and below, the reduction in viral infectivity was significantly greater than the reduction in DNA amplification.[60] Another study comparing the efficacy of three UV wavelengths (224, 254, and 280 nm) emitted by an MP-UV system found that the 260−280 nm wavelength range was most effective at inactivating AdV serotype 2. UV_{224} treatment of AdV resulted in conformational changes in the virus capsid that do not preclude binding to the host cell but prevent one of the subsequent steps of the infection cycle, such as internalization to the cytoplasm, endosomal release, or genome translocation into the host cell nucleus.[86] UV_{254} treatment of viruses also allowed virus−host cell binding, but

https://doi.org/10.1021/acs.est.1c03092
Environ. Sci. Technol. 2021, 55, 16283−16298

it disrupted the viral genome to a greater extent than UV_{224}, although it did not cause modifications in the viral capsid.[86] UV_{280} has a peak due to the absorption of tryptophan and tyrosine amino acids, but it did not seem to inhibit viral binding association with the host cell either and showed a higher capacity than that of UV_{254} to disrupt mRNA transcription under similar applied fluences.[60,86] By targeting different components of AdV, MP-UV likely created a synergistic inactivation effect and hence was more efficient against AdV than LP-UV alone.[16,56,57,86]

Damage to different components of viruses caused by varying wavelengths has implications for the accuracy of detection methods. Molecular methods are a convenient proposition for enteric virus detection because infectivity assays for quantification are highly dependent on cell lines and can take days to weeks to produce cytopathic effects (CPEs).[32,41,83] Long-range qPCR (LR-qPCR) has been previously used for viral quantification after UV damage[29,60,87] and has been shown to give similar results for infectivity-based methods when using LP-UV.[60] While molecular methods are sensitive and precise, they are only effective in detecting damage to their specific molecular target. Beck et al. compared cell infectivity assays to LR-qPCR by using LP-UV and NIST lasers tuned to emit light monochromatically and tested every 10 nm from 210 to 290 nm.[60] They found that there was no significant difference between the two detection methods when the LP-UV was applied at 270, 280, and 290 nm. However, there were highly significant differences at 210, 220, 240, and 260 nm with ANCOVA p-values ranging from 1.4×10^{-4} to 2.6×10^{-9} in the slope coefficient (k), and in all cases in which there was a significant difference between detection methods except for 260 nm, LR-qPCR underestimated the inactivation.[60] This finding illustrates that molecular-based methods are able to detect viruses without infectivity and/or naked DNA/RNA. Integrated cell culture-quantitative PCR (ICC-qPCR) overcomes some of the limitations of qPCR by combining infectivity and nucleic acid detection and can be performed in 2 days to detect the disinfection of enteric viruses.[55] Nevertheless, some discrepancies in enteric virus inactivation between ICC-qPCR, ICC-RT-qPCR, and cell culture-based methods have been reported when using LP-UV, MP-UV, and UV-LED.[32,55,63,88]

In addition to MP-UV, the combination of UV_{254} and oxidative radical promoters (e.g., H_2O_2, TiO_2) can also cause chemical modifications in the tertiary and quaternary structures of proteins and lead to changes in the extent of the hydrophobicity, pH, protein unfolding, and protein cross-linking, which in turn increases susceptibility to protease cleavage.[89] In the UV/H_2O_2 system in clean water, HO• radicals are the dominant radical. The photolysis of H_2O_2 will generate primary radicals (HO•), and then, the primary radical will react with the water to yield secondary radicals.[90] Sun et al. concluded that the disinfection efficacy[91] among different radicals decreased from HO• > CO_3^- > O^{2-}/H_2O as a result of different second-order rate constants toward amino acids.[90] In AOP, the primary mechanism of virus inactivation by HO• radicals is not yet fully understood. Inactivation might be due to damage to the capsid protein, the genome, or a combination of both. For instance, a study suggested that enhanced AdV inactivation using HO• radicals was due to capsid damage and not to DNA damage.[29] Generally, HO• is considered nonspecific, meaning that all amino acids are susceptible to HO• radical degradation during AOP inactivation.[92] However, proteins are reportedly more susceptible to radical-induced cleavage, particularly for specific amino acids such as proline.[93,94] Therefore, viruses with high levels of proline in their protein capsids may be more susceptible to UV/H_2O_2, although further experiments and explorations of other amino acids should be conducted to confirm this hypothesis. The number of related studies examining the use of UV-AOP to inactivate enteric viruses remains limited for thorough meta-data analysis.

Despite studies highlighting that the coupling of a chemical disinfectant such as H_2O_2 can generate radicals that facilitate damage to viral capsids and improve disinfection efficiency in single studies,[29] the UV dose required to reach a 4-$\log_{10}$ reduction in combination with 10 mg/L H_2O_2 in that study was not significantly lower than that of LP-UV inactivation of AdV2 determined in this critical review (p-value = 0.112). The lower UV fluence needed when coupling the disinfectant with H_2O_2 indicated that lower energy is now needed to operate the UV lamps. However, the economic savings can be depleted by the costs incurred for chemical disinfectants. The current market price of hydrogen peroxide (70% by weight) listed by global producers is marked at approximately $0.08 to $1.60 U.S. per L. By contrast, the average cost of electricity is only approximately $0.13/kWh in the U.S.

Similarly, another form of AOP, which includes the combination of UV-C and TiO_2 to disinfect water of viruses, did not significantly reduce the dose needed to disinfect MNV.[40] An earlier study showed significant improvements in using TiO_2 when using UV light in the UV-A (320−400 nm) and UV-B (290−320 nm) ranges,[95] although this approach was not included in our analysis due to the low disinfection efficiency of UV light in this range. To exemplify this finding, in their study, less than a one $\log_{10}$ reduction in MNV was achieved when using UV-A alone after 1500 mJ/cm^2. Further using their data, a 363 mJ/cm^2 dose would be needed for a 4-$\log_{10}$ reduction of MNV. This result contrasts with our study suggesting a 26 mJ/cm^2 minimum dose to achieve a 4-$\log_{10}$ reduction of MNV using LP-UV (Table 1). Adding 1 g/L of TiO_2 made UV-A viricidal, although approximately 1400 mJ/cm^2 was required, while no significant improvement was observed in the case of UV-B supplemented with the same TiO_2 concentration.[95] The increase in inactivation efficacy with UV-A was presumed to be due to the photocatalytic reaction of TiO_2, which generates reactive oxygen species (ROS), such as O^{2-} and HO radicals, that can destroy and damage the viral capsid protein and genome.[96,97] This observation shows that the fluence needed to generate ROS is higher than what is needed to achieve a 4-$\log_{10}$ reduction using LP-UV alone. Thus, there was an increase in energy consumption and electrical costs as well as the need for TiO_2 photocatalysts when using UV/TiO_2, which might preclude it from use in practical applications in full-scale reactors due to the associated costs. Furthermore, the OH radicals generated through UV/TiO_2 may not be homogeneous throughout the bulk solutions and were perhaps instead polarized on the TiO_2 surfaces. This characteristic limits the reaction kinetics and does not justify the increase in operational costs for limited improvements in disinfection efficacy. These observations suggest that using AOP for the sole purpose of inactivating viruses may not be economical, although using AOP to disinfect and remove a wide range of contaminants, including bacteria, viruses, and pharmaceutical compounds, may justify the additional costs.[98−101]

https://doi.org/10.1021/acs.est.1c03092
Environ. Sci. Technol. 2021, 55, 16283−16298

4.3. Comparison of Data with Earlier Review. Overall, our meta-analysis study showed that the order of lower sensitivity among enteric viruses to UV fluence is as follows: Adenoviridae > rotavirus (Reoviridae) > Caliciviridae > Picornaviridae, which is largely consistent with but now expands upon results shown by a previous review,[102] as summarized in Figure S1. Our FCV linear regression coefficient (0.136) is slightly higher than that previously mentioned by Hijnen et al. (0.106).[102] This change in k results in a lower suggested dose; in our case, 29 mJ/cm^2 compared to the 38 mJ/cm^2 required for a 4-log reduction in FCV. This difference may be caused by the different criteria used to source the references; for example, the previous review included a study using UV-B irradiation[103] as well as a single data point from another reference,[104] and in this critical review, we included a study published after this previous review.[38]

Despite for FCV, our regressions lead to similar suggestions for the required LP-UV dose for a 4-log$_{10}$ reduction when examining the same virus and serotype. Our analysis of HAV showed a slightly larger regression coefficient value compared to Hijnen et al.'s results (0.210 and 0.181), and this discrepancy may again be due to differences in the selection criteria for data sets. In this study, unlike the earlier review by Hijnen et al., we did not include results from conference proceedings. However, the difference in the suggested dose for a 4-log$_{10}$ reduction is just 3 mJ/cm^2. For CVB5, in which the data set came from the same references, our UV dose suggestion for a 4-log$_{10}$ reduction was again different by just 3 mJ/cm^2. Our result for RV is also consistent with the previous review, at 0.107 in our critical review compared to 0.102 in theirs, which results in a 1 mJ/cm^2 difference in the dose suggestion for a 4-log$_{10}$ reduction in RV despite clarity in establishing the start of the tailing behavior observed with RV. This tailing inactivation behavior observed with rotavirus SA-11 has resulted from either viral aggregation or/and the presence of a resistant subpopulation.[54,102] Likewise, our PV linear regression coefficient result (0.141) is consistent with the Hijnen study (0.135), again within a 1.2 mJ/cm^2 difference for a 4-log$_{10}$ reduction,[102] despite the inclusion of two references in this critical review that were not included in the previous review.[48,49] Furthermore, the UV fluence needed to achieve a 4-log$_{10}$ reduction in PV as obtained by our linear regression analysis is still within the range of 17−37 mJ/cm^2 reported by IUVA news.[105]

This critical review did not provide distinct linear regressions for each individual paper, as was presented in the Hijnen review.[102] However, a statistical analysis using ANCOVA was performed to establish factors that might affect the inactivation rates and therefore the suggested doses required for a 4-log$_{10}$ reduction of specific viruses. In data sets in which more than one paper, water matrix, or detection/quantification method was used across a single serotype, each of the three factors was tested for statistical significance. For a given factor, all the differing components were compared using pairwise comparisons against each other as well as individually against the rest of the data. These findings showed that the authors were the biggest significant factor rather than the detection methods (i.e., CPE, plaque formation, qPCR, ICC-RT-qPCR, etc.) or water matrices (MWW, DW, MEM, PBS, etc.) (Supporting Information, Text 1). Multiple cases of independent studies using the same water matrix, detection method, virus type and serotype achieving significant differences in disinfection kinetics highlight the need for more studies using enteric viruses so that meta-analyses can provide a more accurate consensus on the efficiency of a given technology against specific serotypes.

5. PERSPECTIVE

5.1. More Studies Are Needed to Evaluate Enteric Virus Inactivation in Treated Wastewater Matrices. While collating the literature for this study, we observed that the majority of the papers demonstrating enteric virus inactivation used phosphate buffer solution and buffered demand-free water or groundwater, with relatively fewer studies using treated wastewater matrices. This information is needed to understand how the water quality affects the inactivation efficiencies for different enteric viruses, particularly when oxidative radical promoters are coupled to UV light. Turbidity-causing materials such as natural organic matter (NOM), total suspended solids, biological particles, inorganic nitrogen, iron salts (primarily ferric iron), and manganese are important constituents that affect the UV disinfection efficacy.[66] For example, Fe(III) has a UV transmittance (measurement of how well UV-C will penetrate a given water or liquid) of ∼100% at 0.2 NTU, which decreases to 38% at 5 NTU.[106] The presence of natural organic matter (NOM) was found to enhance the formation of rotavirus aggregates, especially in the presence of divalent cations.[107] It also appears that viruses can form aggregates around/within particles upon association with organic matter.[108−110] For example, human norovirus and rotavirus may bind to the histo-blood group antigen (HBGA)-like substance produced by bacteria, which functions as a shield against disinfectants.[55] Humic acids can also decrease UV transmittance to 47% at 5 NTU.[106] The lower UV transmittance will therefore reduce the fluence to which viruses are exposed. In addition, humic acid and activated sludge floc particles (particles with size <2 μm) shielded MS2 and T4 bacteriophages from UV disinfection (80 mJ/cm^2) compared to the controls.[111] NH_4^+/NH_3 and NO_2^- can also inhibit UVA/TiO_2 disinfection by reducing the production of hydroxyl radicals in the water matrix.[112]

In treated wastewater, the concentrations of Fe(III), natural organic matter, humic acids, and nitrogenous compounds can vary depending on the type of wastewater treatment technology. For example, wastewater cleaned by an anaerobic membrane bioreactor (AnMBR), an emerging technology that employs anaerobic fermentation and membrane separation processes to remove organics, has a higher nitrogenous concentration than treated water from conventional treated wastewater[113] and may require substantial concentrations of oxidative radical promoters in concert with UV radiation to achieve an effective log reduction[114] of enteric viruses. Likewise, the different operating conditions of conventional activated sludge processes, for example, longer hydraulic and sludge retention times, would also affect the concentrations of organics and inorganics in the final treated wastewater. Given that water quality can affect disinfection efficacies, more systematic studies should be performed to assess how different human enteric viruses behave in response to UV disinfection in various types of treated wastewater that have markedly different water qualities than buffer or drinking water.

5.2. Need for More Studies Evaluating Enteric Virus Inactivation by Emerging UV Technologies. While briefly covered in this critical review, more studies determining the inactivation kinetics of different enteric viruses upon exposure to UV-AOP and UV-LEDs are needed to determine their

https://doi.org/10.1021/acs.est.1c03092
Environ. Sci. Technol. 2021, 55, 16283−16298

comparative efficiency under varying circumstances compared to MP-UV and LP-UV. In addition to finding only two papers on treating enteric viruses with UV-AOP fulfilling our selection criteria, one on MNV[40] and one on AdV2,[29] some of the potential benefits of UV-AOP could have been overlooked due to the sensitivity of many enteric viruses to UV treatments alone. All of the enteric viruses covered in this critical review, in addition to adenovirus serotypes, required <70 mJ/cm^2 during LP-UV treatment (Table 1), suggesting that the added oxidative damage potential of radical generation is unlikely to be significant or necessary. A study on bacteriophage MS2 using a noncytotoxic range of UV light (290−400 nm) showed that adding H_2O_2 only had a significant effect after 230 mJ/cm^2 when using 10 and 25 mg/L H_2O_2,[96] and in the context of this critical review, this level of exposure would only be relevant for AdV41. Furthermore, neither of the AOP studies were performed in water matrices such as municipal wastewater, in which another potential advantage of UV-AOP could be highlighted. The generation of hydroxyl radicals throughout AOP can not only lead to viral damage and disinfection but can also improve water quality by degrading organic micropollutants that are prevalent in wastewater.

Light-emitting diodes have practical advantages due to their small size. Multiple LEDs can be designed to emit light at specific wavelengths and angles and are less limited by their physical size than when they could be installed in a treatment train.[64,115] Although the relatively small sample size of studies (four) using UV-LEDs on enteric viruses covered in this critical review showed a general reduction in the UV dose (mJ/cm^2) compared to LP-UV, the low lamp energy efficiency indicates that they can require up to 90-fold more energy to achieve the same $\log_{10}$-reduction of AdV2.[63] Furthermore, the wavelengths provided by the authors of previous studies are nominal peak wavelengths and do not correspond exactly to actual peak wavelengths. Hence, users of UV-LED need to be especially cautious in determining the best optimal wavelength to use for inactivating enteric viruses.

There are practical advantages of using enteric virus surrogates, such as bacteriophages, both in terms of experimental and regulatory implementation. However, despite the availability of data on using these emerging UV technologies on these surrogates, high variability was found in terms of sensitivity, not only for virus stains but also serotypes, as shown in this critical review, suggesting that there is still a need for kinetic data on enteric viruses to evaluate the applicability of these UV-based technologies thoroughly.

SUMMARY

In summary, our critical review provides the following insights:

(i) MP-UV required 28% of the LP-UV dose to achieve a 4-$\log_{10}$ reduction in AdV2.

(ii) On the basis of the limited number of enteric virus inactivation studies that use UV-AOP, it was observed that the addition of TiO_2 did not significantly enhance the inactivation efficiency compared to LP-UV and MP-UV, and the addition of H_2O_2 requires further validation.

(iii) On the basis of the limited number of enteric virus inactivation studies that use UV-LED, UV-LED at 260 or 280 nm provided a slight improvement compared to LP-UV but not to MP-UV.

(iv) Even among the most resistant enteric viruses evaluated in this study (AdV), there was a 112% increase in the UV dose (mJ/cm^2) required to achieve a 4-$\log_{10}$ reduction between the most susceptible (AdV2/5) and resistant (AdV41) serotypes. A slight difference in the UV dose is also observed among the serotypes of EV and CVB, although more metadata is needed for these two enteric viruses. Hence, on the basis of current observations, the genetic structure alone may not be enough to classify or predict a virus's sensitivity to UV radiation accurately.

(v) Other factors that might affect enteric virus inactivation rates include water matrix, detection/quantification method, and interlaboratory groups, with the last factor playing the biggest significant factor.

(vi) More studies that provide the inactivation kinetics of various types of enteric viruses by UV-AOP and UV-LED are needed to facilitate metadata analysis to provide a more accurate consensus for the efficiency of these two UV-based technologies.

(vii) More studies are also needed to assess how different human enteric viruses would be inactivated in the presence of treated wastewater generated from different types of treatment technologies and hence with different water quality parameters.

ASSOCIATED CONTENT

Supporting Information

The Supporting Information is available free of charge at https://pubs.acs.org/doi/10.1021/acs.est.1c03092.

(PDF)

AUTHOR INFORMATION

Corresponding Author

Pei-Ying Hong − *Water Desalination and Reuse Center (WDRC) and Biological and Environmental Science Division (BESE), King Abdullah University of Science and Technology (KAUST), Thuwal 23955-6900, Saudi Arabia;* orcid.org/0000-0002-4474-6600; Phone: +966 12 8082218; Email: peiying.hong@kaust.edu.sa

Authors

Nicolas Augsburger − *Water Desalination and Reuse Center (WDRC), King Abdullah University of Science and Technology (KAUST), Thuwal 23955-6900, Saudi Arabia*

Andri Taruna Rachmadi − *Water Desalination and Reuse Center (WDRC), King Abdullah University of Science and Technology (KAUST), Thuwal 23955-6900, Saudi Arabia*

Noor Zaouri − *Water Desalination and Reuse Center (WDRC), King Abdullah University of Science and Technology (KAUST), Thuwal 23955-6900, Saudi Arabia*

Yunho Lee − *School of Earth Science and Environmental Engineering, Gwangju Institute and Technology (GIST), Gwangju 61005, Republic of Korea;* orcid.org/0000-0001-5923-4897

Complete contact information is available at: https://pubs.acs.org/10.1021/acs.est.1c03092

Notes

The authors declare no competing financial interest.

https://doi.org/10.1021/acs.est.1c03092
Environ. Sci. Technol. 2021, 55, 16283−16298

■ ACKNOWLEDGMENTS

This study was supported by the KAUST Center Applied Research Funding FCC/1/1971-32-01, Center of Excellence for NEOM Research flagship projects REI/1/4178-03-01, and KAUST Translation Fund REI/1/4223-01-01 awarded to P.Y.-H.

■ REFERENCES

(1) *Transforming our World: The 2030 Agenda for Sustainable Development*; Department of Economic and Social Affairs, United Nations: New York, 2015.
(2) Contaminant Candidate List 4-CCL 4. *U.S. Environmental Protection Agency*. https://www.epa.gov/ccl/contaminant-candidate-list-4-ccl-4-0 (March 30, 2021).
(3) Fong, T.-T.; Lipp, E. K. Enteric viruses of humans and animals in aquatic environments: health risks, detection, and potential water quality assessment tools. *Microbiol. Mol. Biol. Rev.* **2005**, *69* (2), 357−371.
(4) Wyn-Jones, A.; Sellwood, J. Enteric viruses in the aquatic environment. *J. Appl. Microbiol.* **2001**, *91* (6), 945−962.
(5) Crook, J.; Bull, R.; Collins, H.; Cotruvo, J.; Jakubowski, W. *Examining the Criteria for Direct Potable Reuse: Recommendations of an NWRI Independent Advisory Panel*; National Water Research Institute: Fountain Valley, CA, 2013.
(6) Soller, J. A.; Eftim, S. E.; Nappier, S. P. Direct potable reuse microbial risk assessment methodology: Sensitivity analysis and application to State log credit allocations. *Water Res.* **2018**, *128*, 286−292.
(7) *Water Treatment Manual : Disinfection*. U.S. Environmental Protection Agency, 2011.
(8) *Alternative Disinfectant and Oxidants*. U.S. Environmental Protection Agency, 1999.
(9) Richardson, S. D.; Plewa, M. J.; Wagner, E. D.; Schoeny, R.; DeMarini, D. M. Occurrence, genotoxicity, and carcinogenicity of regulated and emerging disinfection by-products in drinking water: a review and roadmap for research. *Mutat. Res., Rev. Mutat. Res.* **2007**, *636* (1−3), 178−242.
(10) Li, X.-F.; Mitch, W. A. Drinking water disinfection byproducts (DBPs) and human health effects: multidisciplinary challenges and opportunities. *Environ. Sci. Technol.* **2018**, *52*, 1681−1689.
(11) Richardson, S. D.; Thruston, A. D.; Caughran, T. V.; Chen, P. H.; Collette, T. W.; Floyd, T. L.; Schenck, K. M.; Lykins, B. W.; Sun, G.-r.; Majetich, G. Identification of new ozone disinfection byproducts in drinking water. *Environ. Sci. Technol.* **1999**, *33* (19), 3368−3377.
(12) Von Gunten, U.; Hoigne, J. Bromate formation during ozonization of bromide-containing waters: interaction of ozone and hydroxyl radical reactions. *Environ. Sci. Technol.* **1994**, *28* (7), 1234−1242.
(13) Soltermann, F.; Abegglen, C.; Gotz, C.; Von Gunten, U. Bromide sources and loads in Swiss surface waters and their relevance for bromate formation during wastewater ozonation. *Environ. Sci. Technol.* **2016**, *50* (18), 9825−9834.
(14) Von Gunten, U. Ozonation of drinking water: Part II. Disinfection and by-product formation in presence of bromide, iodide or chlorine. *Water Res.* **2003**, *37* (7), 1469−1487.
(15) Shah, A. D.; Dotson, A. D.; Linden, K. G.; Mitch, W. A. Impact of UV disinfection combined with chlorination/chloramination on the formation of halonitromethanes and haloacetonitriles in drinking water. *Environ. Sci. Technol.* **2011**, *45* (8), 3657−3664.
(16) Eischeid, A. C.; Linden, K. G. Molecular indications of protein damage in adenoviruses after UV disinfection. *Appl. Environ. Microbiol.* **2011**, *77* (3), 1145−1147.
(17) Eischeid, A. C.; Meyer, J. N.; Linden, K. G. UV disinfection of adenoviruses: molecular indications of DNA damage efficiency. *Appl. Environ. Microbiol.* **2009**, *75* (1), 23−28.
(18) Sinha, R. P.; Häder, D.-P. UV-induced DNA damage and repair: a review. *Photochemical & Photobiological Sciences* **2002**, *1* (4), 225−236.
(19) *Ultraviolet Disinfection Guidance Manual for the Final Long Term 2 Enhanced Surface Water Treatment Rule*; EPA 815-R-06-007 2006; U.S. Environmental Protection Agency, 2006.
(20) *Same Goal, Different Approach; Drinking-Water Standards for New Zealand 2005 (revised 2018)*; Ministry of Health, Wellington, New Zealand, 2018.
(21) Lawal, O.; Warne, S. *Comparing DVGW & USEPA UV Drinking Water Regulations*, 2009.
(22) *Guidance on the Use of Ultraviolet (UV) Irradiation for the Disinfection of Public Water Supplies*; Drinking Water Inspectorate: London, 2016.
(23) Sommer, R.; Cabaj, A.; Hirschmann, G.; Haider, T. Disinfection of drinking water by UV irradiation: Basic principles-specific requirements-international implementations. *Ozone: Sci. Eng.* **2008**, *30* (1), 43−48.
(24) *Guidelines for Canadian Drinking Water Quality: Guideline Technical Document — Copper*; Catalogue No, H144-13/13-2019E-PDF; Water and Air Quality Bureau, Healthy Environments and Consumer Safety Branch, Health Canada: Ottawa, Ontario, 2019
(25) NSF Standards for Water Treatment Systems. *U.S. National Sanitation Foundation*. https://www.nsf.org/knowledge-library/standards-water-treatment-systems (accessed December 2021).
(26) Stefan, M. I. *Advanced Oxidation Processes for Water Treatment: Fundamentals and Applications*; IWA Publishing, 2017.
(27) von Gunten, U. Oxidation processes in water treatment: are we on track? *Environ. Sci. Technol.* **2018**, *52* (9), 5062−5075.
(28) Thiruvenkatachari, R.; Vigneswaran, S.; Moon, I. S. A review on UV/TiO 2 photocatalytic oxidation process (Journal Review). *Korean J. Chem. Eng.* **2008**, *25* (1), 64−72.
(29) Bounty, S.; Rodriguez, R. A.; Linden, K. G. Inactivation of adenovirus using low-dose UV/H2O2 advanced oxidation. *Water Res.* **2012**, *46* (19), 6273−6278.
(30) Knight, A.; Haines, J.; Stals, A.; Li, D.; Uyttendaele, M.; Knight, A.; Jaykus, L.-A. A systematic review of human norovirus survival reveals a greater persistence of human norovirus RT-qPCR signals compared to those of cultivable surrogate viruses. *Int. J. Food Microbiol.* **2016**, *216*, 40−49.
(31) Li, D.; Gu, A. Z.; He, M.; Shi, H.-C.; Yang, W. UV inactivation and resistance of rotavirus evaluated by integrated cell culture and real-time RT-PCR assay. *Water Res.* **2009**, *43* (13), 3261−3269.
(32) Ding, N.; Craik, S. A.; Pang, X.; Lee, B.; Neumann, N. F. Assessing UV Inactivation of Adenovirus 41 Using Integrated Cell Culture Real-Time qPCR/RT-qPCR. *Water Environ. Res.* **2017**, *89* (4), 323−329.
(33) Ettayebi, K.; Crawford, S. E.; Murakami, K.; Broughman, J. R.; Karandikar, U.; Tenge, V. R.; Neill, F. H.; Blutt, S. E.; Zeng, X.-L.; Qu, L.; Kou, B.; Opekun, A. R.; Burrin, D.; Graham, D. Y.; Ramani, S.; Atmar, R. L.; Estes, M. K. Replication of human noroviruses in stem cell−derived human enteroids. *Science* **2016**, *353* (6306), 1387−1393.
(34) Microbial Contaminants − CCL 4. *U.S. Environmental Protection Agency*. https://www.epa.gov/ccl/microbial-contaminants-ccl-4 (March 30, 2021).
(35) Troeger, C.; Blacker, B. F; Khalil, I. A; Rao, P. C; Cao, S.; Zimsen, S. R.; Albertson, S. B; Stanaway, J. D; Deshpande, A.; Abebe, Z.; Alvis-Guzman, N.; Amare, A. T; Asgedom, S. W; Anteneh, Z. A.; Antonio, C. A. T; Aremu, O.; Asfaw, E. T.; Atey, T. M.; Atique, S.; Avokpaho, E. F. G A.; Awasthi, A.; Ayele, H. T.; Barac, A.; Barreto, M. L; Bassat, Q.; Belay, S. A.; Bensenor, I. M; Bhutta, Z. A; Bijani, A.; Bizuneh, H.; Castaneda-Orjuela, C. A; Dadi, A. F.; Dandona, L.; Dandona, R.; Do, H. P.; Dubey, M.; Dubljanin, E.; Edessa, D.; Endries, A. Y.; Eshrati, B.; Farag, T.; Feyissa, G. T.; Foreman, K. J; Forouzanfar, M. H; Fullman, N.; Gething, P. W; Gishu, M. D.; Godwin, W. W; Gugnani, H. C.; Gupta, R.; Hailu, G. B.; Hassen, H. Y.; Hibstu, D. T.; Ilesanmi, O. S; Jonas, J. B; Kahsay, A.; Kang, G.; Kasaeian, A.; Khader, Y. S.; Khalil, I. A; Khan, E. A.; Khan, M. A.;

Khang, Y.-H.; Kissoon, N.; Kochhar, S.; Kotloff, K. L; Koyanagi, A.; Kumar, G A.; Magdy Abd El Razek, H.; Malekzadeh, R.; Malta, D. C.; Mehata, S.; Mendoza, W.; Mengistu, D. T.; Menota, B. G.; Mezgebe, H. B.; Mlashu, F. W.; Murthy, S.; Naik, G. A; Nguyen, C. T.; Nguyen, T. H.; Ningrum, D. N. A.; Ogbo, F. A.; Olagunju, A. T.; Paudel, D.; Platts-Mills, J. A; Qorbani, M.; Rafay, A.; Rai, R. K.; Rana, S. M; Ranabhat, C. L.; Rasella, D.; Ray, S. E; Reis, C.; Renzaho, A. M.; Rezai, M. S.; Ruhago, G. M.; Safiri, S.; Salomon, J. A; Sanabria, J. R.; Sartorius, B.; Sawhney, M.; Sepanlou, S. G; Shigematsu, M.; Sisay, M.; Somayaji, R.; Sreeramareddy, C. T; Sykes, B. L; Taffere, G. R.; Topor-Madry, R.; Tran, B. X.; Tuem, K. B.; Ukwaja, K. N.; Vollset, S. E.; Walson, J. L; Weaver, M. R; Weldegwergs, K. G.; Werdecker, A.; Workicho, A.; Yenesew, M.; Yirsaw, B. D.; Yonemoto, N.; El Sayed Zaki, M.; Vos, T.; Lim, S. S; Naghavi, M.; Murray, C. J.; Mokdad, A. H; Hay, S. I; Reiner, R. C Estimates of the global, regional, and national morbidity, mortality, and aetiologies of diarrhoea in 195 countries: a systematic analysis for the Global Burden of Disease Study 2016. *Lancet Infect. Dis.* **2018**, *18* (11), 1211−1228.

(36) Bolton, J. R.; Linden, K. G. Standardization of methods for fluence (UV dose) determination in bench-scale UV experiments. *J. Environ. Eng.* **2003**, *129* (3), 209−215.

(37) Linden, K. G.; Darby, J. L. Estimating effective germicidal dose from medium pressure UV lamps. *J. Environ. Eng.* **1997**, *123* (11), 1142−1149.

(38) Park, G.; Linden, K.; Sobsey, M. Inactivation of murine norovirus, feline calicivirus and echovirus 12 as surrogates for human norovirus (NoV) and coliphage (F+) MS2 by ultraviolet light (254 nm) and the effect of cell association on UV inactivation. *Lett. Appl. Microbiol.* **2011**, *52* (2), 162−167.

(39) Weng, S.; Dunkin, N.; Schwab, K. J.; McQuarrie, J.; Bell, K.; Jacangelo, J. G. Infectivity reduction efficacy of UV irradiation and peracetic acid-UV combined treatment on MS2 bacteriophage and murine norovirus in secondary wastewater effluent. *J. Environ. Manage.* **2018**, *221*, 1−9.

(40) Lee, J.; Zoh, K.; Ko, G. Inactivation and UV disinfection of murine norovirus with TiO2 under various environmental conditions. *Appl. Environ. Microbiol.* **2008**, *74* (7), 2111−2117.

(41) Thurston-Enriquez, J. A.; Haas, C. N.; Jacangelo, J.; Riley, K.; Gerba, C. P. Inactivation of feline calicivirus and adenovirus type 40 by UV radiation. *Appl. Environ. Microbiol.* **2003**, *69* (1), 577−582.

(42) Tian, P.; Yang, D.; Quigley, C.; Chou, M.; Jiang, X. Inactivation of the Tulane virus, a novel surrogate for the human norovirus. *J. Food Prot.* **2013**, *76* (4), 712−718.

(43) Chang, J. C.; Ossoff, S. F.; Lobe, D. C.; Dorfman, M. H.; Dumais, C. M.; Qualls, R. G.; Johnson, J. D. UV inactivation of pathogenic and indicator microorganisms. *Appl. Environ. Microbiol.* **1985**, *49* (6), 1361−1365.

(44) Gerba, C. P.; Gramos, D. M.; Nwachuku, N. Comparative inactivation of enteroviruses and adenovirus 2 by UV light. *Appl. Environ. Microbiol.* **2002**, *68* (10), 5167−5169.

(45) Harris, G. D.; Adams, V. D.; Sorensen, D. L.; Curtis, M. S. Ultraviolet inactivation of selected bacteria and viruses with photoreactivation of the bacteria. *Water Res.* **1987**, *21* (6), 687−692.

(46) Meng, Q. S.; Gerba, C. P. Comparative inactivation of enteric adenoviruses, poliovirus and coliphages by ultraviolet irradiation. *Water Res.* **1996**, *30* (11), 2665−2668.

(47) Shin, G.-A.; Linden, K. G.; Sobsey, M. D. Low pressure ultraviolet inactivation of pathogenic enteric viruses and bacteriophages. *J. Environ. Eng. Sci.* **2005**, *4* (S1), S7−S11.

(48) Simonet, J.; Gantzer, C. Inactivation and genome degradation of poliovirus 1 and F-specific RNA phages by UV irradiation at 254 nm. *Appl. Environ. Microbiol.* **2006**, *72* (12), 7671−7677.

(49) Woo, H.; Beck, S. E.; Boczek, L. A.; Carlson, K. M.; Brinkman, N. E.; Linden, K. G.; Lawal, O. R.; Hayes, S. L.; Ryu, H. Efficacy of inactivation of human enteroviruses by dual-wavelength germicidal ultraviolet (UV-C) light emitting diodes (LEDs). *Water* **2019**, *11* (6), 1131.

(50) Thompson, S. S.; Jackson, J. L.; Suva-Castillo, M.; Yanko, W. A.; El Jack, Z.; Kuo, J.; Chen, C. L.; Williams, F. P.; Schnurr, D. P. Detection of infectious human adenoviruses in tertiary-treated and ultraviolet-disinfected wastewater. *Water Environ. Res.* **2003**, *75* (2), 163−170.

(51) Sommer, R.; Weber, G.; Cabaj, A.; Wekerle, J.; Keck, G.; Schauberger, G. UV-inactivation of microorganisms in water. *Int. J. Hyg. Environ. Med.* **1989**, *189* (3), 214−224.

(52) Maier, A.; Tougianidou, D.; Wiedenmann, A.; Botzenhart, K. Detection of poliovirus by cell culture and by PCR after UV disinfection. *Water Sci. Technol.* **1995**, *31* (5−6), 141−145.

(53) Battigelli, D.; Sobsey, M.; Lobe, D. The inactivation of hepatitis A virus and other model viruses by UV irradiation. *Water Sci. Technol.* **1993**, *27* (3−4), 339−342.

(54) Nasser, A.; Paulman, H.; Sela, O.; Ktaitzer, T.; Cikurel, H.; Zuckerman, I.; Meir, A.; Aharoni, A.; Adin, A. UV disinfection of wastewater effluents for unrestricted irrigation. *Water Sci. Technol.* **2006**, *54* (3), 83−88.

(55) Gerrity, D.; Ryu, H.; Crittenden, J.; Abbaszadegan, M. UV inactivation of adenovirus type 4 measured by integrated cell culture qPCR. *J. Environ. Sci. Health, Part A: Toxic/Hazard. Subst. Environ. Eng.* **2008**, *43* (14), 1628−1638.

(56) Linden, K. G.; Thurston, J.; Schaefer, R.; Malley, J. P. Enhanced UV inactivation of adenoviruses under polychromatic UV lamps. *Appl. Environ. Microbiol.* **2007**, *73* (23), 7571−7574.

(57) Linden, K. G.; Shin, G. A.; Lee, J. K.; Scheible, K.; Shen, C.; Posy, P. Demonstrating 4-log adenovirus inactivation in a medium-pressure UV disinfection reactor. *J. - Am. Water Works Assoc.* **2009**, *101* (4), 90−99.

(58) Baxter, C. S.; Hofmann, R.; Templeton, M. R.; Brown, M.; Andrews, R. C. Inactivation of adenovirus types 2, 5, and 41 in drinking water by UV light, free chlorine, and monochloramine. *J. Environ. Eng.* **2007**, *133* (1), 95−103.

(59) Sirikanchana, K.; Shisler, J. L.; Marinas, B. J. Effect of exposure to UV-C irradiation and monochloramine on adenovirus serotype 2 early protein expression and DNA replication. *Appl. Environ. Microbiol.* **2008**, *74* (12), 3774−3782.

(60) Beck, S. E.; Rodriguez, R. A.; Linden, K. G.; Hargy, T. M.; Larason, T. C.; Wright, H. B. Wavelength dependent UV inactivation and DNA damage of adenovirus as measured by cell culture infectivity and long range quantitative PCR. *Environ. Sci. Technol.* **2014**, *48* (1), 591−598.

(61) Rattanakul, S.; Oguma, K.; Sakai, H.; Takizawa, S. Inactivation of viruses by combination processes of UV and chlorine. *Journal of Water and Environment Technology* **2014**, *12* (6), 511−523.

(62) Ko, G.; Cromeans, T. L.; Sobsey, M. D. UV inactivation of adenovirus type 41 measured by cell culture mRNA RT-PCR. *Water Res.* **2005**, *39* (15), 3643−3649.

(63) Beck, S. E.; Ryu, H.; Boczek, L. A.; Cashdollar, J. L.; Jeanis, K. M.; Rosenblum, J. S.; Lawal, O. R.; Linden, K. G. Evaluating UV-C LED disinfection performance and investigating potential dual-wavelength synergy. *Water Res.* **2017**, *109*, 207−216.

(64) Oguma, K.; Rattanakul, S.; Bolton, J. R. Application of UV Light−Emitting Diodes to adenovirus in water. *J. Environ. Eng.* **2016**, *142* (3), 04015082.

(65) Oguma, K. Inactivation of feline calicivirus using ultraviolet light-emitting diodes. *FEMS microbiology letters* **2018**, *365* (18), fny194.

(66) Kowalski, W. *Ultraviolet Germicidal Irradiation Handbook: UVGI for Air and Surface Disinfection*; Springer Science & Business Media, 2010.

(67) Oguma, K.; Rattanakul, S.; Masaike, M. Inactivation of health-related microorganisms in water using UV light-emitting diodes. *Water Sci. Technol.: Water Supply* **2019**, *19* (5), 1507−1514.

(68) Oguma, K.; Kita, R.; Sakai, H.; Murakami, M.; Takizawa, S. Application of UV light emitting diodes to batch and flow-through water disinfection systems. *Desalination* **2013**, *328*, 24−30.

(69) Song, K.; Mohseni, M.; Taghipour, F. Application of ultraviolet light-emitting diodes (UV-LEDs) for water disinfection: A review. *Water Res.* **2016**, *94*, 341−349.

https://doi.org/10.1021/acs.est.1c03092
Environ. Sci. Technol. 2021, 55, 16283−16298

(70) Song, K.; Taghipour, F.; Mohseni, M. Microorganisms inactivation by continuous and pulsed irradiation of ultraviolet light-emitting diodes (UV-LEDs). *Chem. Eng. J.* **2018**, *343*, 362−370.
(71) Nguyen, T. M. H.; Suwan, P.; Koottatep, T.; Beck, S. E. Application of a novel, continuous-feeding ultraviolet light emitting diode (UV-LED) system to disinfect domestic wastewater for discharge or agricultural reuse. *Water Res.* **2019**, *153*, 53−62.
(72) Wigginton, K. R.; Pecson, B. M.; Sigstam, T. r.; Bosshard, F.; Kohn, T. Virus inactivation mechanisms: impact of disinfectants on virus function and structural integrity. *Environ. Sci. Technol.* **2012**, *46* (21), 12069−12078.
(73) Wigginton, K. R.; Kohn, T. Virus disinfection mechanisms: the role of virus composition, structure, and function. *Curr. Opin. Virol.* **2012**, *2* (1), 84−89.
(74) Rockey, N.; Young, S.; Kohn, T.; Pecson, B.; Wobus, C. E.; Raskin, L.; Wigginton, K. R. UV Disinfection of human norovirus: evaluating infectivity using a genome-wide PCR-based approach. *Environ. Sci. Technol.* **2020**, *54* (5), 2851−2858.
(75) Ma, H.; Huang, X.; Kang, K.; Li, X.; Tang, X.; Ren, Y.; Wang, Y.; Zhao, G.; Xu, B. Recombination in human coxsackievirus B5 strains that caused an outbreak of viral encephalitis in Henan, China. *Arch. Virol.* **2013**, *158* (10), 2169−2173.
(76) Qiao, Z.; Ye, Y.; Chang, P. H.; Thirunarayanan, D.; Wigginton, K. R. Nucleic acid photolysis by UV254 and the impact of virus encapsidation. *Environ. Sci. Technol.* **2018**, *52* (18), 10408−10415.
(77) Henle, W.; Liu, O. C.; Finter, N. B. Studies on host-virus interactions in the chick embryo-influenza virus system. IX. The period of liberation of virus from infected cells. *J. Exp. Med.* **1954**, *100* (1), 53−70.
(78) Uhnoo, I.; Wadell, G.; Svensson, L.; Johansson, M. Importance of enteric adenoviruses 40 and 41 in acute gastroenteritis in infants and young children. *J. Clin. Microbiol.* **1984**, *20* (3), 365−372.
(79) Kalyuzhniy, O.; Di Paolo, N. C.; Silvestry, M.; Hofherr, S. E.; Barry, M. A.; Stewart, P. L.; Shayakhmetov, D. M. Adenovirus serotype 5 hexon is critical for virus infection of hepatocytes in vivo. *Proc. Natl. Acad. Sci. U. S. A.* **2008**, *105* (14), 5483−5488.
(80) Silver, L.; Anderson, C. W. Interaction of human adenovirus serotype 2 with human lymphoid cells. *Virology* **1988**, *165* (2), 377−387.
(81) Middleton, C. T.; de La Harpe, K.; Su, C.; Law, Y. K.; Crespo-Hernández, C. E.; Kohler, B. DNA excited-state dynamics: from single bases to the double helix. *Annu. Rev. Phys. Chem.* **2009**, *60*, 217−239.
(82) Görner, H. New trends in photobiology: Photochemistry of DNA and related biomolecules: Quantum yields and consequences of photoionization. *J. Photochem. Photobiol., B* **1994**, *26* (2), 117−139.
(83) Guo, H.; Chu, X.; Hu, J. Effect of Host Cells on Low- and Medium-Pressure UV Inactivation of Adenoviruses. *Appl. Environ. Microbiol.* **2010**, *76* (21), 7068.
(84) Pinon, A.; Vialette, M. Survival of Viruses in Water. *Intervirology* **2019**, *61* (5), 214−222.
(85) Cliver, D. O. Capsid and infectivity in virus detection. *Food Environ. Virol.* **2009**, *1* (3−4), 123.
(86) Vazquez-Bravo, B.; Gonçalves, K.; Shisler, J. L.; Mariñas, B. J. Adenovirus replication cycle disruption from exposure to polychromatic ultraviolet irradiation. *Environ. Sci. Technol.* **2018**, *52* (6), 3652−3659.
(87) Rodríguez, R.; Bounty, S.; Linden, K. Long-range quantitative PCR for determining inactivation of adenovirus 2 by ultraviolet light. *J. Appl. Microbiol.* **2013**, *114* (6), 1854−1865.
(88) Araud, E.; Fuzawa, M.; Shisler, J. L.; Li, J.; Nguyen, T. H. UV inactivation of rotavirus and Tulane virus targets different components of the virions. *Appl. Environ. Microbiol.* **2020**, *86* (4), na DOI: 10.1128/AEM.02436-19.
(89) Rule Wigginton, K.; Menin, L.; Montoya, J. P.; Kohn, T. Oxidation of virus proteins during UV254 and singlet oxygen mediated inactivation. *Environ. Sci. Technol.* **2010**, *44* (14), 5437−5443.
(90) Sun, P.; Tyree, C.; Huang, C.-H. Inactivation of Escherichia coli, bacteriophage MS2, and Bacillus spores under UV/H2O2 and UV/peroxydisulfate advanced disinfection conditions. *Environ. Sci. Technol.* **2016**, *50* (8), 4448−4458.
(91) Sun, P.; Zhang, T.; Mejia-Tickner, B.; Zhang, R.; Cai, M.; Huang, C.-H. Rapid disinfection by peracetic acid combined with UV irradiation. *Environ. Sci. Technol. Lett.* **2018**, *5* (6), 400−404.
(92) Mayer, B. K.; Yang, Y.; Gerrity, D. W.; Abbaszadegan, M. The impact of capsid proteins on virus removal and inactivation during water treatment processes. *Microbiol. Insights* **2015**, *8s2*, MBI.S31441.
(93) Hawkins, C.; Davies, M. EPR studies on the selectivity of hydroxyl radical attack on amino acids and peptides. *J. Chem. Soc., Perkin Trans. 2* **1998**, No. 12, 2617−2622.
(94) Jones, B. J.; Vergne, M. J.; Bunk, D. M.; Locascio, L. E.; Hayes, M. A. Cleavage of peptides and proteins using light-generated radicals from titanium dioxide. *Anal. Chem.* **2007**, *79* (4), 1327−1332.
(95) Lee, J. E.; Ko, G. Norovirus and MS2 inactivation kinetics of UV-A and UV-B with and without TiO2. *Water Res.* **2013**, *47* (15), 5607−5613.
(96) Mamane, H.; Shemer, H.; Linden, K. G. Inactivation of E. coli, B. subtilis spores, and MS2, T4, and T7 phage using UV/H2O2 advanced oxidation. *J. Hazard. Mater.* **2007**, *146* (3), 479−486.
(97) Cho, M.; Chung, H.; Choi, W.; Yoon, J. Linear correlation between inactivation of E. coli and OH radical concentration in TiO2 photocatalytic disinfection. *Water Res.* **2004**, *38* (4), 1069−1077.
(98) Kanakaraju, D.; Glass, B. D.; Oelgemöller, M. Advanced oxidation process-mediated removal of pharmaceuticals from water: A review. *J. Environ. Manage.* **2018**, *219*, 189−207.
(99) Sherchan, S. P.; Snyder, S. A.; Gerba, C. P.; Pepper, I. L. Inactivation of MS2 coliphage by UV and hydrogen peroxide: Comparison by cultural and molecular methodologies. *J. Environ. Sci. Health, Part A: Toxic/Hazard. Subst. Environ. Eng.* **2014**, *49* (4), 397−403.
(100) Rizzo, L.; Malato, S.; Antakyali, D.; Beretsou, V. G.; Đolic, M. B.; Gernjak, W.; Heath, E.; Ivancev-Tumbas, I.; Karaolia, P.; Lado Ribeiro, A. R.; Mascolo, G.; McArdell, C. S.; Schaar, H.; Silva, A. M.T.; Fatta-Kassinos, D. Consolidated vs new advanced treatment methods for the removal of contaminants of emerging concern from urban wastewater. *Sci. Total Environ.* **2019**, *655*, 986−1008.
(101) Byrne, C.; Subramanian, G.; Pillai, S. C. Recent advances in photocatalysis for environmental applications. *J. Environ. Chem. Eng.* **2018**, *6* (3), 3531−3555.
(102) Hijnen, W.; Beerendonk, E.; Medema, G. J. Inactivation credit of UV radiation for viruses, bacteria and protozoan (oo) cysts in water: a review. *Water Res.* **2006**, *40* (1), 3−22.
(103) Duizer, E.; Bijkerk, P.; Rockx, B.; De Groot, A.; Twisk, F.; Koopmans, M. Inactivation of caliciviruses. *Appl. Environ. Microbiol.* **2004**, *70* (8), 4538−4543.
(104) De Roda Husman, A.; Bijkerk, P.; Lodder, W.; van den Berg, H.; Pribil, W.; Cabaj, A.; Gehringer, P.; Sommer, R.; Duizer, E. Calicivirus inactivation by nonionizing (UV-253.7 nm) and ionizing (gamma) radiation. *Appl. Environ. Microbiol.* **2004**, *70*, 5089−5093.
(105) Malayeri, A. H.; Mohseni, M.; Cairns, B.; Bolton, J. R.; Chevrefils, G.; Caron, E.; Barbeau, B.; Wright, H.; Linden, K. G. Fluence (UV dose) required to achieve incremental log inactivation of bacteria, protozoa, viruses and algae. *IUVA News* **2016**, *18* (3), 4−6.
(106) Farrell, C.; Hassard, F.; Jefferson, B.; Leziart, T.; Nocker, A.; Jarvis, P. Turbidity composition and the relationship with microbial attachment and UV inactivation efficacy. *Sci. Total Environ.* **2018**, *624*, 638−647.
(107) Gutierrez, L.; Nguyen, T. H. Interactions between rotavirus and Suwannee River organic matter: aggregation, deposition, and adhesion force measurement. *Environ. Sci. Technol.* **2012**, *46* (16), 8705−8713.
(108) Peduzzi, P.; Weinbauer, M. G. Effect of Concentrating the Virus-Rich 2−200-Nm Size Fraction of Seawater on the Formation of Algal Flocs (Marine Snow) *Limnol. Limnol. Oceanogr.* **1993**, *38* (7), 1562−1565.
(109) Bettarel, Y.; Motegi, C.; Weinbauer, M. G.; Mari, X. Colonization and Release Proceses of Viruses and Prokaryotes on

Artificial Marine Macroaggregates. *FEMS Microbiol. Lett.* **2016**, *363* (1), fnv216.
(110) Weinbauer, M.; Bettarel, Y.; Cattaneo, R.; Luef, B.; Maier, C.; Motegi, C.; Peduzzi, P.; Mari, X. Viral ecology of organic and inorganic particles in aquatic systems: avenues for further research. *Aquat. Microb. Ecol.* **2009**, *57* (3), 321−341.
(111) Templeton, M. R.; Andrews, R. C.; Hofmann, R. Particle-associated viruses in water: impacts on disinfection processes. *Crit. Rev. Environ. Sci. Technol.* **2008**, *38* (3), 137−164.
(112) Zuo, X.; Hu, J.; Chen, M. The role and fate of inorganic nitrogen species during UVA/TiO2 disinfection. *Water Res.* **2015**, *80*, 12−19.
(113) Zaouri, N.; Cheng, H.; Khairunnisa, F.; Alahmed, A.; Blilou, I.; Hong, P.-Y. A type dependent effect of treated wastewater matrix on seed germination and food production. *Sci. Total Environ.* **2021**, *769*, 144573.
(114) Augsburger, N.; Zaouri, N.; Cheng, H.; Hong, P.-Y. The use of UV/H2O2 to facilitate removal of emerging contaminants in anaerobic membrane bioreactor effluents. *Environ. Res.* **2021**, *198*, 110479.
(115) Lui, G. Y.; Roser, D.; Corkish, R.; Ashbolt, N. J.; Stuetz, R. Point-of-use water disinfection using ultraviolet and visible light-emitting diodes. *Sci. Total Environ.* **2016**, *553*, 626−635.

https://doi.org/10.1021/acs.est.1c03092
Environ. Sci. Technol. 2021, 55, 16283−16298